Publication P6

Robert Tenno and Antti Pohjoranta. 2008. Exact controls for the superconformal via fill process. In: Proceedings of the UKACC International Conference on Control 2008. Manchester, UK. 2-4 September 2008. 6 pages.

EXACT CONTROLS FOR THE
SUPERCONFORMAL VIA FILL PROCESS

Robert Tenno [*,1] Antti Pohjoranta [*]

** Helsinki University of Technology (TKK), Control
Engineering, P.O. Box 5500, Espoo, Finland*

Abstract: This paper reports a means for stabilizing the microvia fill ratio on a
desired level, using the total plating time and the system galvanostat setpoint
current density as optimal controls. Both control variables are solved as functions
of the process state as well as selected manufacturer preference variables that are
typical for the via fill technology applied in multilayered printed circuit board
production. The optimal controls are obtained as a system of two equations and
solved numerically with the gradient descent method. Results of the numerical
analysis are presented and discussed.

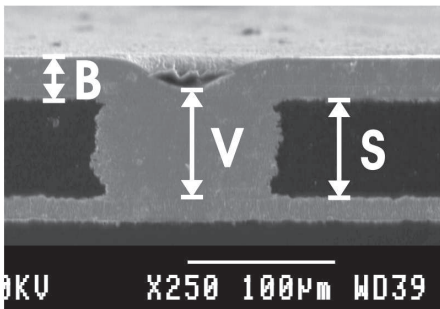Keywords: via fill control, distributed parameters systems control

Figure 1. A microvia cross-section SEM-photograph. The letters indicate: B $= y_B$, V $= y_V$, S $= H$.

1. INTRODUCTION

The microvia fill process is an electrochemical
process in which metallic copper interconnects
are made between adjacent layers of multilayered
printed circuit boards (MLBs) by first drilling
holes on an individual board layer and then filling
these holes with copper electrodeposition.

Superconformal deposit growth at the microvia
domain is obtained by adding specific growth in-
hibiting (suppressor) and enhancing (accelerator)
chemicals, whose concentrations must be well bal-
anced (Andricacos *et al.*, 1998). In practice, these
are regulated at constant levels, while the plating
time and plating current density are operational
parameters, adjusted to obtain a good fill result.
A common measure for the via fill success is the
via fill ratio, r

$$r = \frac{y_V(\tau)}{H + y_B(\tau)} 100\%. \qquad (1)$$

In (1) τ is the plating time (s), y is the deposit
thickness (m) measured vertically in the via bot-
tom center point (y_V) and on the level board
surface (y_B). H is the thickness of the dielectric
board substrate (m). These are illustrated in Fig.
1. The subscripts V and B are used also further
in the text to denote the corresponding locations.

In MLB manufacturing, a common requirement is
$r \geq 80\%$ (denoted R=80% from here on). Also
a thin deposit on the level board is a good fill
characteristic as well as a short fill time, which
directly increases productivity of a plating bath,
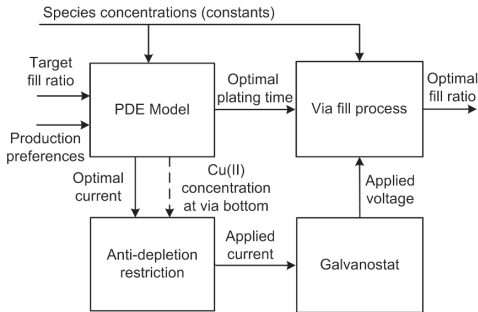
---

[1] robert.tenno@tkk.fi

Figure 2. The control system architecture.

but, which also as a disadvantage increases the risk of deposit failures caused by too high plating current density. The mentioned requirements are accounted for in the following cost function J

$$
\begin{aligned}
J_{i_{target}}^{\tau} = & \left[R \left(H + y_B(\tau) \right) - y_V(\tau) \right]^2 \\
& + k_1 y_B^2(\tau) + k_2 \tau^2
\end{aligned}
\quad (2)
$$

In (2) k_1 is the weight on aiming to obtain a thin deposit on the level board surface and k_2 is the weight on compromising mass-production against risk of deposit failures. The weights are chosen by the manufacturer (thus called the *production preferences*).

Minimization of (2) includes two problems: (i) the deposit growth control problem and (ii) the process stopping control problem. In manual control, these are solved by a process operator. A system developed for automatic via fill control is shown in Fig. 2; the controller minimizes the cost function (2) with respect to a PDE system developed for the via fill process.

The optimal controls (plating time and current density) are evaluated upon the chosen target fill ratio, the control preferences and the included species' concentrations. The optimal current density is limited with a hard restriction or soft limit, to prevent failures caused by Cu(II) ion depletion inside the via. The optimal current density, on which limits are applied is given to the system galvanostat as current density setpoint to be realized by adjusting the voltage between the plating bath electrodes appropriately. The optimal cell voltage and the optimal plating time yield the desired fill ratio at the process output. These ideas along with their mathematical formulation are discussed further.

Thus far the related literature is mainly focused on experimental studies (Dow *et al.*, 2003), (Lefebvre *et al.*, 2003) aiming for bottom-up fill through a good choice additives. In microchip manufacturing the process is extensively studied and modelled (Moffat *et al.*, 2005), (Vereecken *et*

al., 2005), (Akolkar and Landau, 2004), (Gabrielli *et al.*, 2005), (Wheeler *et al.*, 2003) while similar studies for microvias have been reported only few. The via fill control literature is focused on process monitoring and practical realization aspects (Dow *et al.*, 2006), (Dow and Liu, 2006) except for (Tenno and Pohjoranta, 2007), where a simple control method is developed.

The control model applied here bases on the curvature enhanced accelerator accumulation effects (Moffat *et al.*, 2007) documented as a predictive model for the microvia fill process in (Tenno and Pohjoranta, 2008), (Pohjoranta and Tenno, 2007). Although many similar models have been proposed (Moffat *et al.*, 2005), (Vereecken *et al.*, 2005), (Akolkar and Landau, 2004), (Gabrielli *et al.*, 2005), (Wheeler *et al.*, 2003), these are for microchip technology with ca. hundred times smaller vias and significantly shorter plating times, which make application of such models in the microvia fill processes unfeasible.

2. PROBLEM FORMULATION

The control problem is to choose the optimal stopping time to minimize the cost function in (2) with respect to deposit growth on the level board y_B and inside the via y_V. The process is modelled with finite element model, in a 2D, Cartesian changing geometry system, applying the arbitrary Lagrange-Eulerian (ALE) method, as documented thoroughly in (Tenno and Pohjoranta, 2008), (Pohjoranta and Tenno, 2007).

The required deposit thickness value changes are obtained as in (3)-(4).

$$
\begin{cases}
dy_B = \left[\frac{\partial y}{\partial X} dX + \frac{\partial y}{\partial Y} dY \right]_B \\
y_B(0) = 0
\end{cases}
\quad (3)
$$

$$
\begin{cases}
dy_V = \left[\frac{\partial y}{\partial X} dX + \frac{\partial y}{\partial Y} dY \right]_V \\
y_V(0) = -H
\end{cases}
\quad (4)
$$

The differentials $(\partial y / \partial X, \partial y / \partial Y)$ in (3)-(4) are components of the deformation gradient, essential in the ALE method.

The spatial deformation field (i.e. the displacements) is a velocity field solved from the Laplace equation (in a vector form) $\nabla^2 \mathbf{u} = 0$, where $\mathbf{u}$ (m/s) is the 2D velocity vector, $\mathbf{u} = [u, v]^T$, the X-directional velocity being $u = \frac{dx}{dt}$ and the Y-directional velocity $v = \frac{dy}{dt}$.

The model as well as the process behind the control system, where the mentioned variables are obtained from, are documented thoroughly in the cited references and thus, for brevity, only a brief walk through the relevant equations and terms is

given in this proceedings article. (For clarity, wide-spanning equations are collected in Tbl. 1).

2.1 The process model equations

$\mathbf{u} \bullet \mathbf{n}$ on the cathode is determined by the cathode current density i_c (A/m^2), obtained from (7) with (8) in Tbl. 1. Here $\rho = 2F\rho_{Cu}/M_{Cu}$ (2.721 C/m^3), where $M_{Cu} = 0.06355$ kg/mol, $\rho_{Cu} = 8960$ kg/m^3 and $F = 96487$ C/mol. $\mathbf{n}$ is the cathode surface normal vector. i_0 is the Cu(II)/Cu(s) exchange current density (A/m^2), $K = 77.85$ V^{-1}, α_i are apparent transfer coefficients (subscript a for anodic, c for cathodic), E is the driving potential for electrode reaction (V), k_A is the ratio between the anode and cathode areas, μ_i are the proportional coverage of free adsorption sites. c_{Cu} is the Cu(II) ion concentration (mol/m^3), c_{Cu}^0 is 1000 mol/m^3 and c_{Cu}^{lim} 3.5 mol/m^3.

i_c is controlled by a galvanostat that sets E upon a chosen $i_c^B = i_{target}$ (9). However, the current density is limited by mass transfer, a limit approximated here as $i_{lim} = 2Fc_{Cu}^b D_{Cu}/\delta$, where c_{Cu}^b is c_{Cu} in the electrolyte bulk, D_{Cu} is Cu(II) diffusivity (m^2/s) and δ the thickness of the diffusion layer (m). The target current density is admissible if $i_{target} \leq k_g i_{lim}$, $k_g < 1$. The condition assures the upper limit current density (time-variable) inside the via, given in (10).

In the bulk solution, mass transfer of species is modelled with regular mass transfer equations (diffusion and Nernst-Planck w/o electroneutrality) (11) and on the cathode surface with surface mass balance equations (12). $\nabla_T = \mathbf{L} \bullet \nabla$, where $\mathbf{L}$ is a projection operator $\mathbf{L} = \mathbf{I} - \mathbf{n}\mathbf{n}^T$, $\mathbf{I}$ being the identity tensor. $\frac{d\psi}{dt} = T_{inc}(1 - \psi)$, with $\psi(0) = 0$ and $T_{inc} \approx 2000$ s. k_i^c is the the consumption reaction rate coefficient for species i (m/s), D_i is diffusivity (m^2/s) and Γ_i^0 is the maximum surface coverage (mol/m^2). D_i^s is the surface diffusivity for i (m^2/s), k_i^a the adsorption rate (m^3/mol/s), k_i^d the desorption rate (s^{-1}) and c_i the additive i's concentration (mol/m^3).

In (11), the electric potential ϕ satisfies $-\nabla \bullet \sigma\nabla\phi = 0$, with a set voltage on the anodic boundary and i_c on the cathodic boundary. σ is the electric conductivity of the electrolyte, S/m.

2.2 The controls

The optimal current density should be limited before applied as a setpoint for a galvanostat by either of the following modifications:

(1) A *hard restriction* based on a constant mass transfer limit approximation

$$i_{set} = \min\left(i_{target}, k_g i_{lim}^B\right) \qquad (5)$$

(2) A *soft limit*, approximated by using a c_{Cu} measurement on the via bottom (c_{Cu}^V)

$$i_{set} = \frac{c_{Cu}^V}{c_{Cu}^V + c_{Cu}^b/100} \min\left(i_{target}, k_g i_{lim}^B\right) \qquad (6)$$

In (5) and (6) i_{target} is the optimal current density without limitation (A/m^2), i_{set} is the setpoint for galvanostat with limitation (A/m^2) and c_{Cu}^V is the concentration of Cu(II) ions in the via bottom, (mol/m^3).

The former current density i_{set} (in (5)) is recalled further as the hard-limited current and the latter one (in (6)) as the soft-limited current density. The unrestricted current density i_{target} will be found as the optimal control in Section 3.

3. OPTIMAL CONTROLS

The target current density and plating time are fixed constants for a galvanostat. In practice, they are found experimentally for each MLB product; here they are found from the model using either the exhaustive search or a faster iterative method explained below.

The deposition thickness on the level board and in via is expressed with the applied controls by using Faraday's law

$$y_B(\tau, i) = \frac{i}{\rho}\tau, \quad y_V(\tau, i) = \frac{i}{\rho}\int_0^\tau \varphi(t)dt. \qquad (18)$$

In (18) i and τ are the applied controls, the subscript indices from $i_{target}, \tau_{target}$ being omitted from here on to shorten the further formulae. $\varphi(t)$ is the via fill function on the level board and on the via bottom (V and B, respectively) (15).

Minimizing the cost function (2) with respect to the growth processes (18) gives the optimal controls in the following semi-explicit form (19)-(21).

$$i(\tau) = \rho w(\tau), \qquad (19)$$

with the auxiliary function (20)

$$w(\tau) = -HR\frac{\tau R - z(\tau)}{(\tau R - z(\tau))^2 + k_1\tau}, \qquad (20)$$

where $z(\tau)$ is a solution of the equation (21)

$$\frac{dz}{dt} = \varphi(t), \quad z(0) = 0. \qquad (21)$$

The plating time satisfies the nonlinear equation (16).

The solution of (19)-(21) can be found iteratively using a simple gradient descent (GD) method (17).

Table 1. List of wide-spanning equations.

$$i_c = -2i_0 \left(\frac{a_{Cu}}{a_{Cu}^0} \right)^{\frac{\alpha_a(1+\alpha_c)}{\alpha_a+\alpha_c}} \mu_c \left(k_A \frac{\mu_a}{\mu_c} \right)^{\frac{\alpha_c}{\alpha_a+\alpha_c}} \sinh \left(K \frac{\alpha_c \alpha_a}{\alpha_a + \alpha_c} E \right) \tag{7}$$

$$\mu_a = 1, \quad \mu_c = 1 - \theta_{Supp}, \quad \frac{a_{Cu}}{a_{Cu}^0} = \frac{c_{Cu}}{c_{Cu}^0} \left(\frac{c_{Cu} + c_{Cu}^{lim}}{c_{Cu}^0 + c_{Cu}^{lim}} \right)^{-0.5554} \tag{8}$$

$$i_c^V = i_{target} \left\{ \frac{1 - \theta_{Supp}^V}{1 - \theta_{Supp}^B} \left(\frac{c_{Cu}^V}{c_{Cu}^B} \left(\frac{c_{Cu}^V + c_{Cu}^{lim}}{c_{Cu}^B + c_{Cu}^{lim}} \right)^{-0.5554} \right)^{1+\alpha_c} \right\}^{\frac{\alpha_a}{\alpha_a+\alpha_c}} \tag{9}$$

$$i_{lim}^V = k_g i_{lim}^B \left\{ \frac{1 - \theta_{Supp}^V}{1 - \theta_{Supp}^B} \left(\frac{c_{Cu}^V}{c_{Cu}^B} \left(\frac{c_{Cu}^V + c_{Cu}^{lim}}{c_{Cu}^B + c_{Cu}^{lim}} \right)^{-0.5554} \right)^{1+\alpha_c} \right\}^{\frac{\alpha_a}{\alpha_a+\alpha_c}} \tag{10}$$

$$\frac{\partial c_{Supp}}{\partial t} = D_{Supp}\nabla^2 c_{Supp}, \quad \frac{\partial c_{Acc}}{\partial t} = D_{Acc}\nabla^2 c_{Acc} + K D_{Acc} \nabla \bullet (c_{Acc}\nabla\phi)$$

$$\frac{\partial c_{Cu}}{\partial t} = \nabla \bullet (D_{Cu}\nabla c_{Cu}) + K \nabla \bullet (D_{Cu} c_{Cu} \nabla\phi) \tag{11}$$

$$\frac{\partial \theta_{Acc}}{\partial t} + D_{Acc}^s \nabla_T^2 \theta_{Acc} + \mathbf{u}_T \bullet \nabla_T \theta_{Acc} + \theta_{Acc}\mathbf{L} \bullet \nabla \mathbf{u} = k_{Acc}^a c_{Acc}(1 - \theta_{Acc}) - k_{Acc}^d \psi \theta_{Acc}$$

$$\frac{\partial \theta_{Supp}}{\partial t} + D_{Supp}^s \nabla_T^2 \theta_{Supp} + \mathbf{u}_T \bullet \nabla_T \theta_{Supp} + \theta_{Supp}\mathbf{L} \bullet \nabla \mathbf{u} = k_{Supp}^a c_{Supp}(1 - \theta_{Supp} - \theta_{Acc}) - \psi k_{Supp}^d \theta_{Supp} \tag{12}$$

$$D_{Supp}\nabla c_{Supp}(t,x_c,y_c) = k_{Supp}^c c_{Supp} + \Gamma_{Supp}^0 k_{Supp}^a c_{Supp}\psi(1 - \theta_{Supp} - \theta_{Acc}) \tag{13}$$

$$D_{Acc}\nabla c_{Acc}(t,x_c,y_c) = k_{Acc}^c c_{Acc} + \Gamma_{Acc}^0 k_{Acc}^a c_{Acc}\psi(1 - \theta_{Acc}) \tag{14}$$

$$\varphi(t) = \left\{ \frac{1 - \theta_{Supp}^V}{1 - \theta_{Supp}^B} \left(\frac{c_{Cu}^V}{c_{Cu}^B} \left(\frac{c_{Cu}^V + c_{Cu}^{lim}}{c_{Cu}^B + c_{Cu}^{lim}} \right)^{-0.5554} \right)^{1+\alpha_c} \right\}^{\frac{\alpha_a}{\alpha_a+\alpha_c}} \tag{15}$$

$$\tau \left(R(R - \varphi(\tau)) + k_1 + \frac{k_2}{w(\tau)^2} \right) - (R - \varphi(\tau)) \left[z(\tau) - \frac{HR}{w(\tau)} \right] = 0 \tag{16}$$

$$\lambda_{n+1} = \lambda_n - \frac{2}{\rho} \begin{bmatrix} 10^{15} & 0 \\ 0 & 2 \cdot 10^{12} \end{bmatrix} \begin{bmatrix} g(\tau_n, i_n) \\ f(\tau_n, i_n) \end{bmatrix}, \quad n = 0, 1 \ldots \tag{17}$$

In (17) $\lambda = \begin{bmatrix} \tau & i \end{bmatrix}^T$ is the optimal control, similarly as in (18), limited with the hard (5) or soft limit (6). The other functions are standard components of the GD algorithm, i.e. functions (19) and (16) designated here as f and g along with their derivatives, all approximated upon the iterated controls $\tau = \tau_n$, $i = i_n$ as given below.

$$f(\tau_n, i_n) = (R\tau_n - z_n)[R(H + w_n\tau_n) - w_k z_n]$$
$$+ k_1 w_n \tau_n^2$$
$$g(\tau_n, i_n) = i_n(R - \varphi_n)[R(H + w_n\tau_n) - w_n z_n]$$
$$+ \tau_n \rho(k_2 + k_1 w_n^2)$$

4. NUMERICAL ANALYSIS RESULTS

In this section, the optimal controls are discussed and experimented along with hard and soft limits. The target fill ratio was chosen $R = 96\%$.

Above a gradient descent based method was given to find the optimal controls. An exhaustive search method to complete the same is simpler but much more time consuming than the GD method. An interesting result provided by the exhaustive search, however, is the possibility to visualize

the cost function (1) in the neighborhood of the optimal control values. The visualization shows, that the cost function has an "optimum valley", which has a rather level bottom. The GD method finds the valley bottom quickly (5-10 iterations) but in order to locate the exact optimum, several (15-20) more iterations are required to proceed along the valley bottom. If the exact optimum is sought for, an exhaustive search may be feasible. Both methods are applied in this section.

4.1 Optimal controls restricted with hard limits

The fill ratio obtained in simulations depends on plating time as well as applied target current density as shown in Fig. 3(a). The target end-time fill ratio of 96% was reached with all examined plating times. Naturally, the target was reached faster if a larger current density was applied.

In Fig. 3(c) the colors indicate levels of equal cost function value and the four markers show four different optimal controls. The effect of production preferences is evident. For example, if $k_1 = 10^{-7}$, $k_2 = 2 \cdot 10^{-7}$ (Case 2 in Tbl. 2) then the optimal controls are $\tau_{target} = 4220$ s and
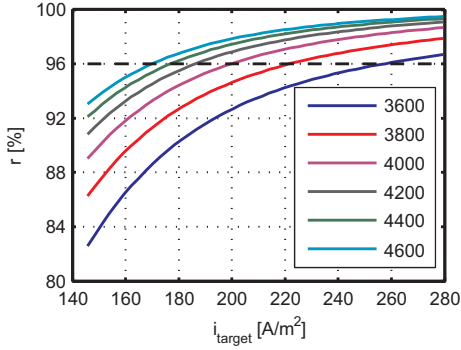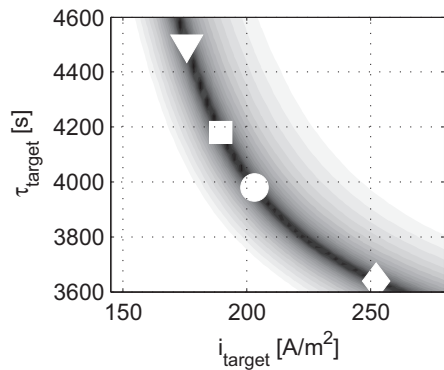
(a) End-time Fill ratio as function hard-limited applied current density, with various plating times.
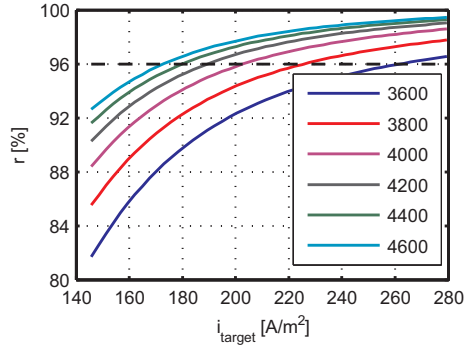
(b) End-point fill ratio as function soft-limited applied current density, with various plating times.
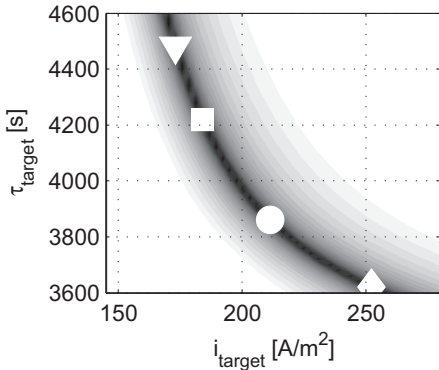
(c) The "optimum valley" of control cost, in terms of plating time and **hard-limited** applied current density. The marked optimal controls are those listed in Table 2.

(d) The "optimum valley" of control cost, in terms of plating time and **soft-limited** applied current density. The marked optimal controls are those listed in Table 3.

Table 2. Optimal controls with hard-limited current.

Case	Preferences		τ_{target}	i_{target}	Marker
n:o	k_1	k_2	(s)	(A/m^2)	
1	10^{-7}	0	4480	173.1	△
2	10^{-7}	$2 \cdot 10^{-10}$	4220	184.0	□
3	0	0	3860	211.3	○
4	0	$2 \cdot 10^{-9}$	3620	252.2	◇

$i_{target} = 184$ A/m^2, correspondingly denoted in the cost function behavior plot in Fig. 3(c) with a square marker. Other points marked in the cost function "optimum valley" are optimal controls corresponding to other preferences k_1 and k_2 (as listed in Tbl. 2).

If $k_1 = 10^{-7}$, $k_2 = 0$ (case 1 in Table 2), then a relatively low current density of 173 A/m^2 and a long plating time of 4480 s are optimal. If $k_1 = 0$, $k_2 = 2 \cdot 10^{-7}$ the situation is opposite and $(i, \tau) = (252$ A/m^2, 3620 s$)$.

If $k_1 = k_2 = 0$, the optimal controls 211 A/m^2 and 3860 sec are not well defined as we will be seen later. The cost function shape is the same for all preferences but the extremum point depends on the chosen preferences.

4.2 Optimal controls restricted with soft limits

Similar results as for hard-limited control current density can be found for the soft-limited control current density. The desired fill ratio of 96% is achieved for all controls as shown in Fig. 3(b).

Table 3. Optimal controls with soft-limited current.

Case	Preferences		τ_{target}	i_{target}	Marker
n:o	k_1	k_2	(s)	(A/m^2)	
1	10^{-7}	0	4500	175.8	△
2	10^{-7}	$2 \cdot 10^{-10}$	4180	189.4	□
3	0	0	3980	203.1	○
4	0	$2 \cdot 10^{-9}$	3640	252.2	◇

Because the soft limitation (6) yields lower current densities than the hard limit, (5) the cost function and its "valley bottom" (Fig. 3(d)) is slightly shifted to the direction of higher current densities and longer plaiting time, compared to that with hard limits (Fig. 3(c)). Generally, also the optimal controls are only slightly shifted but for $k_1 = k_2 = 0$ (case 3) the shift is large, probably due to computational instability created by the, in this case, ill-posed cost function.

Generally, the soft limit increases optimal current density and decreases plating time compared to the hard restriction, the end-time fill ratio remaining nearly the same.

It is known that the microvia fill process behavior is strongly dependent on plating bath conditions. Therefore also optimal controls depend on process variables such as all the species' bulk solution concentrations, which should thus be either stabilized at a chosen setpoint or if not, the optimal controls should be periodically recalculated. Verification of the reported model against practical, empirical data is given in (Pohjoranta and Tenno, 2007), (Tenno and Pohjoranta, 2008) where also a simulation of how the bulk solution Cu(II) ions', suppressor and accelerator additives' concentration affects the fill process output is given. It is shown that the model is adequate in respect to the measured data.

5. CONCLUSION

Though the via fill process along with its model are complex, optimal selections for plating time and system galvanostat setpoint current density can be found. These are controls, coupled with a nonlinear relationship and whose exact location in the time-current plane depend on the production preferences, specifically how important is a thin thickness of deposit on the level board and how important is a short plating period compared to the risk of deposition failures caused by too high plating current density. Without predefined preferences the controls are not well posed; a desired end-time fill ratio alone does not properly define the optimal controls. The performed simulations convince that by running the process with optimally, the target fill ratio is reached at a predicted optimal plating time for each of chosen production preferences.

A hard restriction and soft limit can both be used to prevent Cu(II) ion depletion inside the via, as was tested in the performed experiments. The soft limit moves the increases optimal current density and shortens optimal plating time compared to a hard restriction on current density. The optimal controls depend on the process state and on species' concentrations, whereby these should either be regulated at chosen levels or if not, the optimal controls should be periodically recalculated.

REFERENCES

Akolkar, R. and U. Landau (2004). A time-dependent transport-kinetics model for additive interactions in copper interconnect met-

allization. **151**(11), C702–C711. ISSN 0013-4651.

Andricacos, P. C., C. Uzoh, J. O. Dukovic, J. Horkans and H. Deligianni (1998). Damascene copper electroplating for chip interconnections. **42**(5), 567–574.

Dow, W.-P. and C.-W. Liu (2006). Evaluating the filling performance of a copper plating formula using a simple galvanostat method. **153**(3), C190–C194. ISSN 0013-4651.

Dow, W-P., H-S. Huang and Z. Lin (2003). Interactions between brightener and chloride ions on copper electroplating for laser-drilled via-hole filling. **6**(9), C134–C136. ISSN 1099-0062.

Dow, W.-P., M.-Y. Yen, C.-W. Chou, C.-W. Liu, W.-H. Yang and C.-H. Chen (2006). Practical monitoring of filling performance in a copper plating bath. **9**(8), C134–C137. ISSN 1099-0062.

Gabrielli, C., P. Mocoteguy, H. Perrot, D. Nieto-Sanz and A. Zdunek (2005). A model for copper deposition in the damascene process. **51**(11), 1462–1472. ISSN 0013-4686.

Lefebvre, M., G. Allardyce, M. Seita, H. Tsuchida, M. Kusaka and S. Hayashi (2003). Copper electroplating technology for microvia filling. *Circuit World* **29**(2), 9–14. ISSN 0305-6120.

Moffat, T. P., D. Wheeler, M. D. Edelstein and D. Josell (2005). Superconformal film growth: Mechanism and quantification. **49**(1), 19–36. ISSN 0018-8646.

Moffat, T.P., D. Wheeler, S.-K. Kim and D. Josell (2007). Curvature enhanced adsorbate coverage mechanism for bottom-up superfilling and bump control in damascene processing. **53**(1), 145–154.

Pohjoranta, A. J. and R. Tenno (2007). A method for microvia fill process modelling in a cu-cu-electrode system with additives. **154**(10), D502–D509.

Tenno, R. and A. J. Pohjoranta (2008). An ale model for prediction and control of the microvia fill process with two additives. **155**(5), 123–123.

Tenno, R. and A.J. Pohjoranta (2007). Microvia fill ratio control. IEEE International Symposium on Industrial Electronics 2007, Vigo, Spain.

Vereecken, P. M., R. A. Binstead, H. Deligiani and P. C. Andricacos (2005). The chemistry of additives in damascene copper plating. **49**(1), 3–18. ISSN 0018-8646.

Wheeler, D., D. Josell and T.P. Moffat (2003). Modeling superconformal electrodeposition using the level set method. **150**(5), C302–C310. ISSN 0013-4651.